Contact area calculation between elastic solids bounded by mound rough surfaces

Palasantzas, G

Published in:
Solid State Communications

DOI:
10.1016/S0038-1098(03)00009-7

Publication date:
2003

Available online at www.sciencedirect.com
SCIENCE DIRECT®
PERGAMON
Solid State Communications 125 (2003) 611–615
solid state communications
www.elsevier.com/locate/ssc

Contact area calculation between elastic solids bounded by mound rough surfaces

G. Palasantzas*

Department of Applied Physics, Materials Science Centre, University of Groningen, 9747 AG Groningen, The Netherlands

Received 18 November 2002; accepted 6 January 2003 by J. H. Davies

Abstract

In this work, we investigate the influence of mound roughness on the contact area between elastic bodies. The mound roughness is described by the r.m.s. roughness amplitude w, the average mound separation Λ, and the system correlation length ζ. In general, the real contact area has a complex dependence on the lateral parameters ζ and Λ. As a function of the contact length scale λ, the contact area approaches macroscopic values rather fast for contact lengths $\lambda \geq \Lambda$ and significant system correlation lengths ζ ($\geq \Lambda$). Finally, as a function of the applied load σ_o the contact area increases significantly with increasing load if $\zeta \geq \Lambda$, while for $\zeta \ll \Lambda$ it approaches macroscopic values even for very weak loads ($\ll E$; with E the solid body elastic modulus).

PACS: 81.40.Pq; 62.20. − x

Keywords: A. Surfaces and interfaces; B. Contact mechanics; C. Roughness

Many real surfaces which are encountered in technological applications possess roughness over a wide range of lateral length scales, i.e. from millimetres down to nanometers. As a result when two solid bodies with macroscopically flat surfaces are brought into contact, the real contact area will only be a fraction of the apparent macroscopic contact area. Indeed, the real contact area can be thought as the area composed of asperities of one solid body, which are squeezed against asperities of the other body. These asperities can deform elastically or plastically depending on the material and loading conditions. At any rate, the determination of the real contact area is a fundamental problem with important technological applications, which include heat transfer phenomena between solid bodies, electrical transport, sliding friction, adhesive forces between solid bodies [1–11] etc.

The real contact area can vary non-linearly with the loading force that pushes together two solid bodies. Hertz [12] proved that the contact area of two elastic bodies of quadratic profile varies non-linearly with the loading force F, namely $\propto F^{2/3}$. However, for a fractal rough surface where small spherical humps are distributed on top of larger ones [13], it was found that the real contact area varies linearly with applied load F. A similar conclusion was drawn from other studies where the roughness was approximated with asperities with spherical summits and a Gaussian height distribution [1,2,5]. The approximation of the asperity summits with paraboloids yielded a real contact area, which also varies linearly with weak applied loads [3,4].

The case of random self-affine rough surfaces, which is known to occur for many surfaces and interfaces [14–23], has been also investigated in contact phenomena [6–10]. These studies described calculations of the real contact area for weak applied loads ($\ll E$; with E the elastic modulus), which, in addition, were based on extrapolations between asymptotic limits of the self-affine roughness spectrum. Under these conditions, it was shown that the real contact area $A(\lambda)$ at lateral length scale λ varies as a power law $A(\lambda) \propto \lambda^{1-H}$ [9,10]. The parameter H is the roughness exponent that characterises the degree of surface irregularity

* Tel.: +31-50363-4272-31; fax: +31-50-363-4881.
E-mail address: g.palasantzas@phys.rug.nl (G. Palasantzas).

0038-1098/03/$ - see front matter © 2003 Published by Elsevier Science Ltd.
doi:10.1016/S0038-1098(03)00009-7

at short lateral length scales ($<\xi$; with ξ in-plane roughness correlation length). Further studies have shown that the dependence of the real contact area $A(\lambda)$ on the roughness exponent H is more complex (even for weak applied loads) depending also on the magnitude of the contact length λ with respect the roughness correlation length ξ [24].

So far, the studies with self-affine roughness are limited to roughness exponents $0 < H < 1$, while the case $H = 1$ requires more special attention since it represents a special category of roughness (besides that of the Gaussian roughness described by the correlation function $\sim e^{-(r/\xi)^{2H}}$ with $H = 1$ [21]), which is the mound roughness. Indeed, during film growth on solid substrates, the growth front can be rough in the sense that multilayer step structures are formed [22,24–31]. In this case the existence of an asymmetric step-edge diffusion barrier (Schwoebel barrier) inhibits the down-hill diffusion of incoming atoms leading effectively to the creation of multilayer step structures in the form of mounds [22,24–31]. Examples of mound roughness include the growth of Ag/Ag(111) by Vrijmoeth et al. and Heyvaert et al. [29,30], Cu/Cu(100) by Zuo and Wendelken [28], Fe/Fe(001) by Strocio et al. [27]. In general, if during roughness formation the corresponding dynamic process leads to a particular wavelength selection, the corresponding morphology can be that of mound roughness [22,23]. Therefore, in this work we will investigate the effect of mound interface roughness on the contact area between elastic bodies under conditions of frictionless contact.

Contact theory: For frictionless contact between two elastic solids with rough surfaces, the contact stress depends only on the gap shape between the solids prior to any loading [6–10]. The system can be described by a flat elastic surface of Poisson's ratio ν and elastic modulus E, which is in contact with a rigid body that has a roughness profile which reproduces the same undeformed gap between the surfaces [6–10]. The parameters E and ν are related to the parameters (ν_k, E_k) of the two elastic solids by the relation $(1-\nu^2)/E = \sum_{k=1,2}(1-\nu_k^2)/E_k$. Assuming only elastic deformation ($\sigma_{\text{yield}} = +\infty$), we obtain the ratio of the real contact area $A(\lambda)$ at lateral length scale λ (if the surface was smooth on all length scales shorter than λ) to that of the macroscopic contact area $A(L)$ of size L [6–10] by $P(\lambda) = \int P(\sigma,\lambda)\mathrm{d}\sigma$. $P(\sigma, \lambda)$ is the stress distribution in the contact area with boundary conditions $P(\sigma = 0,\ \lambda) = 0$ and $P(\sigma = +\infty, \lambda) = \infty$. It has been shown that [9,10]

$$P(\lambda) = \frac{2}{\pi}\int_0^{+\infty} x^{-1}\sin x\, e^{-G(\lambda)x^2}\,dx,$$
$$G(\lambda) = \frac{1}{8}\left[\frac{E}{(1-\nu^2)\sigma_o}\right]^2 \int_{2\pi/L<q<2\pi/\lambda} q^2 C(q)\mathrm{d}^2q \quad (1)$$

where σ_o is the applied load, and $C(q)$ is the Fourier transform of the height–height auto correlation function $C(\vec{r}) = \langle h(\vec{r})h(0)\rangle$ with $h(\vec{r})$ the roughness fluctuation so as $\langle h\rangle = 0$. $\langle\ldots\rangle$ stands as an ensemble average over possible roughness configurations.

Roughness model: Calculation of $P(\lambda)$ from Eq. (1) requires the knowledge of $G(\lambda)$ and thus of the roughness spectrum $C(q)$. Mound rough surfaces have been described by the interface roughness amplitude w, the system correlation length ζ that determines how randomly the mounds are distributed on the surface, and the average mound separation Λ [22,31]. In Fourier space the mound morphology can be described by [22,31]

$$C(q) = \frac{1}{(2\pi)}\frac{w^2\zeta^2}{2} e^{-(4\pi^2+q^2\Lambda^2)(\zeta^2/4\Lambda^2)} I_o(\pi q\zeta^2/\Lambda) \quad (2)$$

with $I_o(x)$ the modified Bessel function of first kind and zero order. If $\zeta \ll \Lambda$ the roughness reproduces behaviour close to that of Gaussian roughness which corresponds to roughness exponent $H = 1$. Note that the correlation function $C(r)$ for mound roughness has an oscillatory behaviour for $\zeta \geq \Lambda$ leading to a characteristic satellite ring at $q = 2\pi/\Lambda$ for the roughness spectrum $C(q)$ [31].

Our calculations were performed for macroscopic contact size $L = 100$ μm, Poisson ratio $\nu = 0.3$, and r.m.s. roughness amplitude $w = 1$ nm and $w \leq \Lambda$, ζ (assuming nanometer scale roughness). The roughness amplitude w has a simple effect on the contact area so as its increment leads to contact area decrement because $G(\lambda) \propto w^2$ ($C(q) \propto w^2$), while any complex dependence will arise as a function of the lateral length scales Λ and ζ.

Fig. 1 shows calculations of the ratio $P(\lambda) = A(\lambda)/A(L)$ versus the contact length scale λ for various values of ζ and Λ. For fixed system correlation length ζ and variable mound separation Λ (Fig. 1(a)), $P(\lambda)$ and thus the real contact area $A(\lambda)$ increases with lateral length scale λ and approaches values close to the macroscopic area ($P(\lambda)\approx 1$) for $\lambda > 2\Lambda$ as long as $\zeta < \Lambda < 4\zeta$. For relatively small average mound separations Λ ($<\zeta$), the contact area reaches very fast a macroscopic value. Indeed, as a function of the system correlation length ζ for fixed Λ (Fig. 1(b)), the contact area reaches gradually the macroscopic value if $\zeta \ll \Lambda$, while with increasing ζ the increment of the contact area is limited by the value of the average mound separation Λ.

In order to understand the behaviour of $P(\lambda)$ one has to follow the behaviour of $G(\lambda)$ as a function of ζ and Λ (Fig. 1(c)). From Eqs. (1) and (2) we obtain,

$$G(\lambda) = \frac{1}{8}\left[\frac{E}{(1-\nu^2)\sigma_o}\right]^2 \frac{w^2\varsigma^2}{2} e^{-\pi^2\varsigma^2/\Lambda^2}\int_{2\pi/L}^{2\pi/\lambda} e^{-q^2\zeta^2/4} I_o \times(\pi q\zeta^2/\Lambda)q^3\,dq. \quad (3)$$

Eq. (3) indicates that for $\zeta > \Lambda$ the presence of the exponential factor $e^{-\pi^2\zeta^2/\Lambda^2}$ will diminish faster $G(\lambda)$ (Fig. 1(c)) and thus will lead faster to a macroscopic value for the contact area ($P(\lambda)\sim 1$). For the case of Gaussian roughness

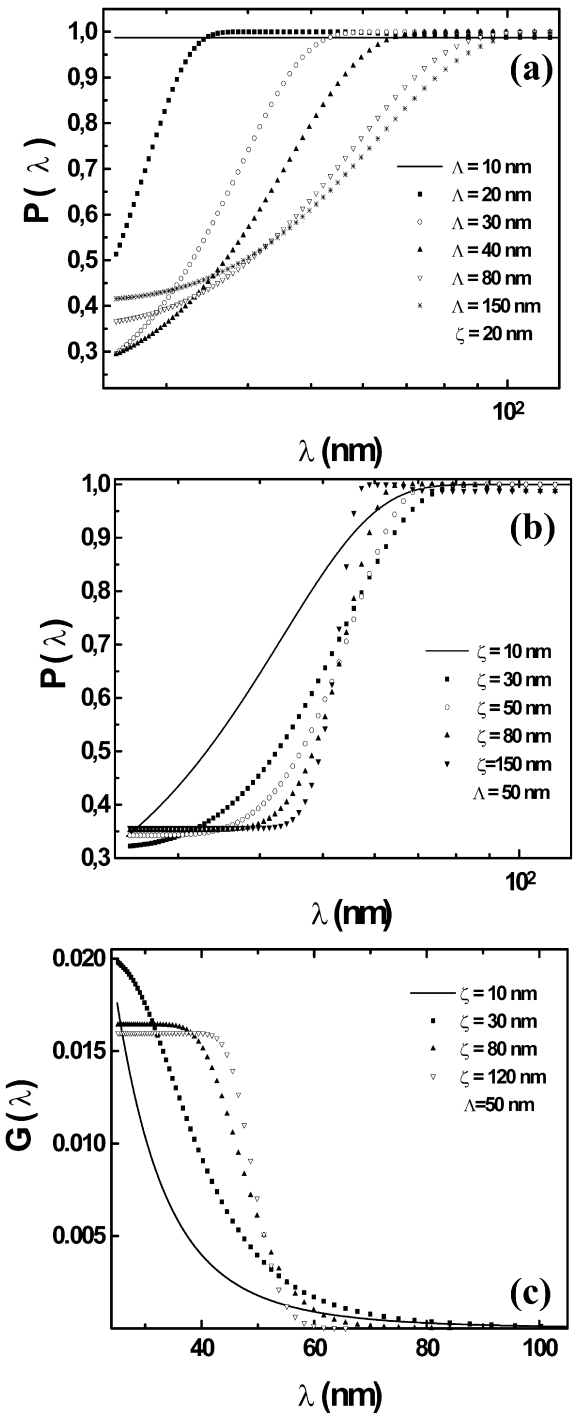

Fig. 1. (a) $P(\lambda)$ vs. λ for fixed ζ and various values of Λ as indicated. (b) $P(\lambda)$ vs. λ for fixed Λ and various values of ζ as indicated. (c) Roughness factor $G(\lambda)$ vs. lateral length scale λ as in (b). In all cases we assumed relatively weak loads $E/\sigma_o = 30$.

or $\Lambda \gg \zeta$, we obtain the simple analytic result

$$G(\lambda) = \left[\frac{E}{(1-\nu^2)\sigma_o}\right]^2 \frac{w^2}{2\zeta^2} \times \left[e^{-\pi^2\zeta^2/L^2}\left(1+\pi^2\frac{\zeta^2}{L^2}\right) - e^{-\pi^2\zeta^2/\lambda^2}\left(1+\pi^2\frac{\zeta^2}{\lambda^2}\right)\right]. \quad (4)$$

For $\lambda \ll \zeta$, Eq. (4) yields the asymptotic value $G(\lambda \ll \varsigma) \cong [E/(1-\nu^2)\sigma_o]^2(w^2/2\varsigma^2)$ which is independent of the contact length scale λ. In the opposite limit $\lambda \gg \zeta$, we obtain the simple result $G(\lambda \ll \varsigma) \cong [E/(1-\nu^2)\sigma_o]^2(w^2/2\zeta^2)(\pi^4\varsigma^4)\times(\lambda^{-4} - L^{-4})$ with $\lambda \leq L$.

Furthermore, if we plot $P(\lambda)$ as a function of the average mound separation Λ (Fig. 2(a)) a rather complex behaviour develops where the contact area has values close to the macroscopic one for $\lambda \gg \zeta$. However, for ζ comparable or

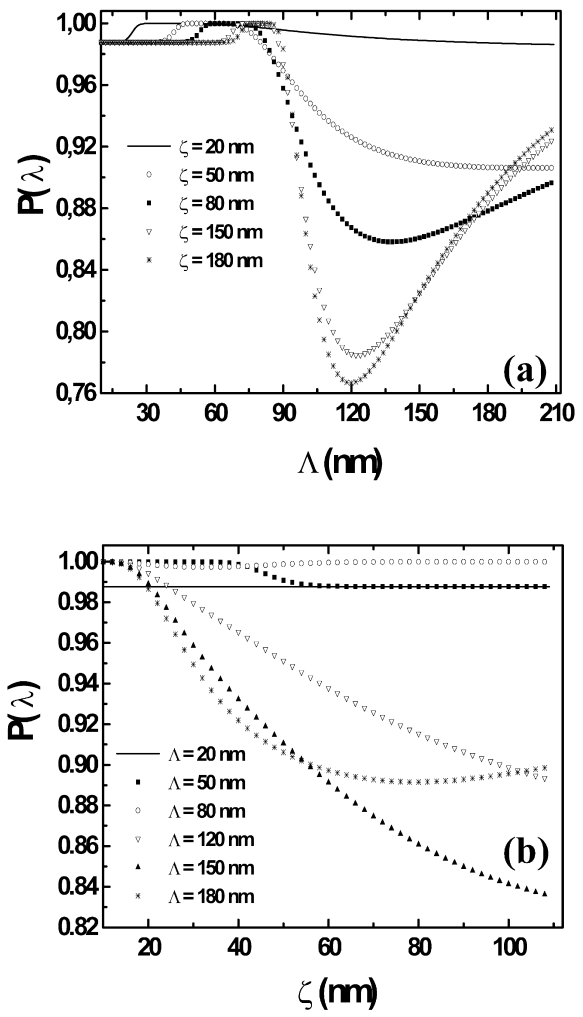

Fig. 2. (a) $P(\lambda)$ vs. Λ for various values of ζ as indicated. (b) $P(\lambda)$ vs. ζ for various values of Λ as indicated. In both cases we used $E/\sigma_o = 30$, and $\lambda = 100$ nm.

larger than the contact length λ, the ratio $P(\lambda)$ and thus the contact area $A(\lambda)$ decreases with further increment of the average mound separation Λ. Similar complicated situation is revealed for $P(\lambda)$ as a function of the system correlation length ζ for various mound separations Λ shown in Fig. 2(b). Physically, as the average mound separation Λ increases the ratio λ/Λ (for fixed contact length λ) decreases which favours lowering of the contact area, while increment of Λ (for fixed roughness amplitude w) leads to surface smoothening which favours larger contact area. The competition between these processes lead to the minimum observed in Fig. 2(a) for large system correlation lengths ζ ($\approx \lambda$). However, for $\zeta \ll \lambda$ there is no any minimum and the contact area decreases with increasing mound separation Λ.

Up to now we have considered rather weak applied loads so that $E/\sigma_o = 30$ in order to focus mainly on the morphology effects. Next, we investigate the dependence of $P(\lambda)$ on the applied load σ_o. As Fig. 3(a) indicates, for average mound separations Λ smaller than the system correlation length ζ, the contact area has a macroscopic value even for very weak loads ($\sigma_o \ll E$) where linear behaviour is expected [9,10]. For weak loads ($\sigma_o \ll E$) and $G(\lambda) \gg 1$ we obtain $P(\lambda) \approx 1/\sqrt{\pi G(\lambda)}$ which yields $P(\lambda) \propto \sigma_o/E$ since $G(\lambda) \propto [E/\sigma_o]^2$ [9,10]. Furthermore, with increasing average mound separation Λ so that $\Lambda > \zeta$, the linear regime starts to appear for $\sigma_o \ll E$, and saturation (contact area with macroscopic value) commences for higher loads with increasing Λ up to the point $\Lambda \approx \lambda$. Fig. 3(b) shows in more detail the effect of the applied σ_o for $\Lambda = \zeta$ where clearly saturation occurs very fast (for contact length scales $\lambda > \Lambda$) for high applied loads in the range $0.1 < \sigma_o/E < 1$.

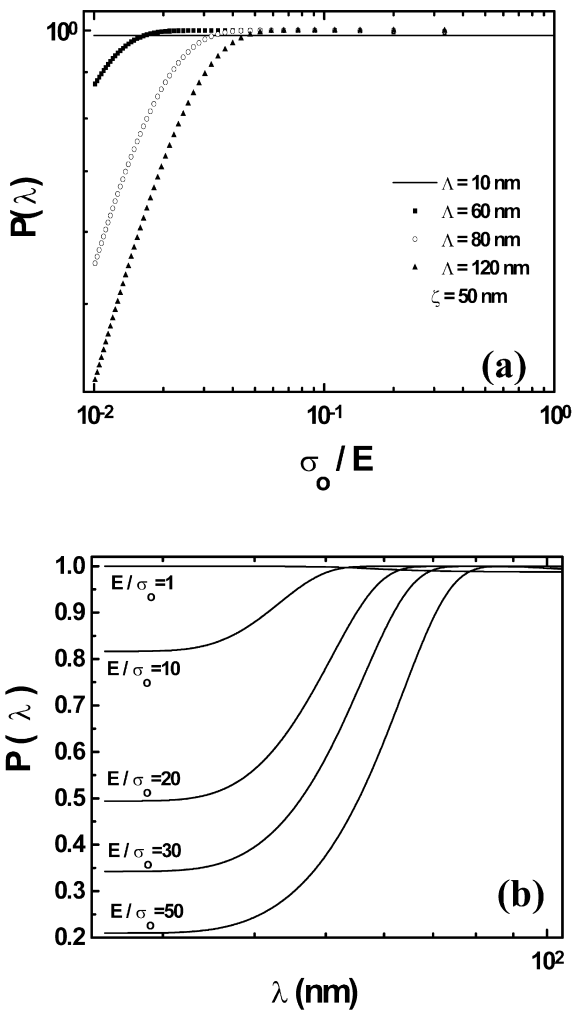

Fig. 3. (a) $P(\lambda)$ vs. σ_o/E for $\zeta = 50$ nm, $\lambda = 100$ nm, and various values of Λ as indicated. (b) $P(\lambda)$ vs. contact length λ for $\Lambda = \zeta = 50$ nm and various values of E/σ_o.

In conclusion, we investigated the influence of mound roughness on the real contact area between elastic bodies bounded by rough surfaces. The mound roughness is described by the r.m.s. roughness amplitude w, the average mound separation Λ, and the system correlation length ζ. In general the real contact area has a complex dependence on the morphology parameters ζ and Λ. As a function of the contact length scale λ, the contact area approaches macroscopic values rather fast for contact lengths $\lambda \geq \Lambda$ and significant system correlation lengths $\zeta \geq \Lambda$. Finally, as a function of the applied load σ_o the contact area increases significantly with increasing applied load for $\zeta \geq \Lambda$, while for $\zeta \ll \Lambda$ it approaches macroscopic values even for very weak loads ($\ll E$).

Acknowledgements

I would like to acknowledge support from the Nederlandse Organisatie voor Wetenschappelijk Onderzoek (NWO).

References

[1] J.A. Greenwood, in: I.L. Singer, H.M. Polack (Eds.), Fundamentals of Friction, Macroscopic and Microscopic Processes, Kluwer, Dordrecht, 1992.
[2] J.A. Greenwood, J.B.P. Williamson, Proc. R. Soc. London Ser. A 295 (1966) 300.
[3] A.W. Bush, R.D. Gibson, T.R. Thomas, Wear 35 (1975) 87.
[4] A.W. Bush, R.D. Gibson, G.P. Keogh, Mech. Res. Commun. 3 (1976) 169.
[5] K.L. Jonhson, Contact Mechanics, Cambridge University Press, Cambridge, 1985.
[6] B.N.J. Persson, Phys. Rev. Lett. 87 (2001) 1161.
[7] B.N.J. Persson, E. Tosatti, J. Chem. Phys. 115 (2001) 5597.
[8] S. Zilberman, B.N.J. Persson, Solid State Commun. 123 (2002) 173.
[9] B.N.J. Persson, F. Bucher, B. Chiaia, Phys. Rev. B 65 (2002) 184106.
[10] B.N.J. Persson, Eur. Phys. J. E8 (2002) 385.

[11] B.N.J. Persson, Sliding friction: Physical Principles and Applications, Second ed., Springer, Heidelberg, 2000.
[12] H. Hertz, J. Reine, Angew. Math. 92 (1882) 156.
[13] J.F. Archard, Proc. R. Soc. London, Ser. A 243 (1957) 190.
[14] J. Krim, G. Palasantzas, Int. J. Mod. Phys. B 9 (1995) 599 see page 605 for Ag/Ag(111) system.
[15] P. Meakin, Fractals, Scaling, and Growth far from Equilibrium, Cambridge University Press, Cambridge, 1998.
[16] F. Family, T. Viscek, Dynamics of Fractal Surfaces, World Scientific, Singapore, 1991.
[17] For various self-affine roughness correlation models see also.G. Palasantzas, Phys. Rev. B 48 (1993) 14472.
[18] For various self-affine roughness correlation models see also.G. Palasantzas, Phys. Rev. B 49 (1994) 5785.
[19] For various self-affine roughness correlation models see also.G. Palasantzas, J. Krim, Phys. Rev. B 48 (1993) 2873.
[20] For various self-affine roughness correlation models see also.G. Palasantzas, Phys. Rev. E 49 (1994) 1740.
[21] For various self-affine roughness correlation models see also. S.K. Sinha, E.B. Sirota, S. Garoff, H.B. Stanley, Phys. Rev. B 38 (1988) 2297.
[22] Y.P. Zhao, G.-C. Wang, T.-M. Lu, Characterization of amorphous and crystalline rough surfaces—principles and applications, Experimental Methods in the Physical Science, vol. 37, Academic Press, 2000, See page 43 for a discussion of mound roughness for the system Cu/Cu(100).
[23] A.-L. Barabási, H.E. Stanley, Fractal Concepts in Surface Growth, Cambridge University Press, Cambridge, 1995.
[24] G. Palasantzas, J.Th.M. De Hosson, Phys. Rev. E (2003) in press.
[25] M.D. Johnson, et al., Phys. Rev. Lett. 72 (1994) 116.
[26] M. Siegert, M. Plischke, Phys. Rev. Lett. 73 (1994) 1517.
[27] J.A. Stroscio, et al., Phys. Rev. Lett. 75 (1995) 4246 Growth of Fe/Fe(001).
[28] J.-K. Zuo, J.F. Wendelken, Phys. Rev. Lett. 78 (1997) 2791 Growth of Cu/Cu(100)0.
[29] J. Vrijmoeth, et al., Phys. Rev. Lett. 72 (1994) 3843 Growth of Ag/Ag(111).
[30] I. Heyvaert, et al., Phys. Rev. E 54 (1996) 349 Growth of Ag/Ag(111).
[31] Y.-P. Zhao, H.-Y. Yang, G.C. Wang, T.-M. Lu, Phys. Rev. B 57 (1998) 1922.